Loss of cortical control over the descending pain modulatory system determines the development of the neuropathic pain state in rats

Authors: Drake RAR[1], Steel KAJ[2], Apps R[1], *Lumb BM[1], *Pickering AE[1,3]

Affiliation: 1 - School of Physiology, Pharmacology & Neuroscience, University of Bristol, UK. 2 – School of Biosciences, University of Cardiff, UK. 3 - Bristol Anaesthesia, Pain & Critical Care Sciences, Bristol Medical School, Bristol Royal Infirmary, Bristol, BS2 8HW.

Contributions: *These authors were jointly senior. We have used the CRediT Taxonomy for contributor roles. Conceptualization: RARD, BML and AEP; Methodology: RARD, BML, AEP; Formal Analysis: RARD & AEP; Investigation: RARD and KAJS; Resources: AEP, BML and RA; Writing – original draft: RARD; Writing – review and editing: RARD, AEP, BML and RA; Visualization: RARD, KAJS and AEP; Supervision: AEP, BML, RA and RARD; Project Administration: RARD; Funding Acquisition: BML, RARD, AEP and RA.

Acknowledgements: We would like to thank Mrs Rachel Bissett for her assistance with histological processing and the Wolfson Bioimaging Facility for their support and assistance with image acquisition. We would like to thank Dr Eric J Kremer for his kind gift of CAV-CMV-CRE, and Dr Brian Roth and Dr Karl Deisseroth for the supply of viral vectors used in this work. This work was supported by the Medical Research Council Grant number MR/P00668/X1.

Correspondence: Robert Drake - Robert.drake@bristol.ac.uk, Biomedical Science Building, University Walk, University of Bristol, BS8 1TD.

Abstract:

The loss of descending inhibitory control is thought critical to the development of chronic pain but what causes this loss in function is not well understood. We have investigated the dynamic contribution of prelimbic cortical neuronal projections to the periaqueductal grey (PrL-P) to the development of neuropathic pain in rats using combined opto- and chemo-genetic approaches. We found PrL-P neurons to exert a tonic inhibitory control on thermal withdrawal thresholds in uninjured animals. Following nerve injury, ongoing activity in PrL-P neurons masked latent hypersensitivity and improved affective state. However, this function is lost as the development of sensory hypersensitivity emerges. Despite this loss of tonic control, opto-activation of PrL-P neurons at late post-injury timepoints could restore the anti-allodynic effects by inhibition of spinal nociceptive processing. We suggest that the loss of cortical drive to the descending pain modulatory system underpins the expression of neuropathic sensitisation after nerve injury.

Introduction:

There is a pressing need to better understand the causal mechanisms of chronic pain and develop effective therapeutic strategies that will alleviate its societal burden (Breivik *et al.*, 2006). The brain, as opposed to the periphery, has received increasing focus as a critical contributor to chronic pain development (Ossipov, Dussor and Porreca, 2010; Denk, McMahon and Tracey, 2014; Baliki and Apkarian, 2015). The descending pain modulatory system (DPMS) links brain and spinal cord to provide potent and targeted regulation of nociceptive processing at multiple levels of the neuroaxis, including the spinal dorsal horn (Millan, 2002; Tracey and Mantyh, 2007). Importantly, the DPMS can affect the perception of pain and is a critical regulator of the development of the pain state following injury (Eippert *et al.*, 2009; Hughes *et al.*, 2013; Drake *et al.*, 2014; Hirschberg *et al.*, 2017).

Typically, following acute injury, this descending regulation functions to inhibit spinal dorsal horn circuits that that subserve damaged tissue and, in doing so, moderates central sensitisation (Vanegas and Schaible, 2004; Drake *et al.*, 2014). However, net loss of inhibitory control has been noted in a wide variety of human chronic pain disorders and descending inhibitory systems are depleted and non-functional in animal models of persistent pain (Yarnitsky, 2010; Hughes *et al.*, 2013, 2015; Staud, 2013; Bannister *et al.*, 2015). Similarly, trait deficiencies in endogenous inhibitory control and/or its engagement by peripheral injury are thought to impart individual vulnerability to chronic pain (Edwards, 2005; Yarnitsky, 2010; Granovsky, 2013; Denk, McMahon and Tracey, 2014; González-Roldán *et al.*, 2020). What causes this deficit / loss in function of the DPMS is not well understood but could help identify critical and generalisable mechanisms of chronic pain development that lay the foundation for the development of more effective therapeutic strategies.

In humans, the medial prefrontal cortex (mPFC) displays specific activity related to acute pain processing, pain expectation and endogenous pain modulation (Lorenz *et al.*, 2002; Wager *et al.*, 2004; Wiech and Tracey, 2009; Legrain *et al.*, 2011; Brooks, Davies and Pickering, 2017). Importantly, the mPFC shows alterations in structure and function that are related to and, sometimes, predictive of the

transition to chronic pain (Apkarian *et al.*, 2004; Baliki *et al.*, 2006, 2012). Direct corticofugal projections from the mPFC to the midbrain link it to the DPMS to provide a route to pain state regulation (An *et al.*, 1998; Huang *et al.*, 2019). The midbrain periaqueductal grey (PAG) is a core component of the DPMS able to facilitate and/or inhibit spinal nociceptive processing via pain modulatory brainstem nuclei including the rostral ventromedial medulla and locus coeruleus (Mantyh, 1983; Waters and Lumb, 2008; Ossipov, Dussor and Porreca, 2010; Drake *et al.*, 2016). Notably, altered functional connectivity between the mPFC and PAG is observed in human patients with musculoskeletal, neuropathic and inflammatory chronic pain suggesting that altered cortical control may contribute to maladaptation of the DPMS and that this mechanism may be relevant to chronic pain in general (Cifre *et al.*, 2012; Yu *et al.*, 2014; Chen *et al.*, 2017; Mills *et al.*, 2018; Segerdahl *et al.*, 2018).

Recently, preclinical investigation has demonstrated the prelimbic cortex (PrL), a division of the rodent mPFC, is able to affect noxious thresholds in neuropathic rats (Huang *et al.*, 2019). However, whether the role of PrL neurons that target the PAG (PrL-P) in sensory and/or affective aspects of the pain state are dynamically altered during development of neuropathic pain is not known. To assess this question we transfected PrL-P neurons with excitatory optogenetic and inhibitory chemogenetic actuator proteins to allow selective manipulation of their activity (Zhang *et al.*, 2010; Sternson and Roth, 2014). This enabled their contribution to sensory and affective aspects of pain-like behaviour to be charted before and, at regular intervals, following peripheral nerve injury in rats. We also used electrophysiological methods to investigate whether PrL-P neurons exert effects on spinal dorsal horn nociceptive circuit activity to establish whether these effects are mediated by descending control.

Methods:

Animals

All experimental and surgical procedures were conducted in accordance with the UK Animals (Scientific Procedures) Act (1998) and local ethical review. Adult male Wistar rats (n=56, 250-275g, Envigo, NL) were housed in the University of Bristol's Animal Service Unit with cage enrichment (e.g. cardboard tubes, wooden chews), on a reversed light cycle and with food/water provided ad libitum. Where possible animals were grouped house but were singly housed for up to seven days while healing from surgery occurred.

Experimental Design

This study's primary objective was to investigate the contribution of PrL-P neurons to the development of sensory and affective aspects of neuropathic pain. To achieve this, opto- and chemogenic actuator proteins were expressed in PrL-P neurons to enable interrogation of the behavioural and neurophysiological consequences of their selective and specific opto-activation and chemo-inhibition. To selectively express actuator proteins in only PrL-P afferents we used an intersectional, Cre-dependent viral vector approach (Boender *et al.*, 2014). 12 animals were used to develop the intersectional viral vector methodology in vivo. Briefly, cre-dependent adenoviral vectors encoding Channelrhodopsin2(ChR2) or the inhibitory DREADD, hM4Di, were delivered to the PrL. To restrict their expression to only those PrL neurons that project to the PAG we delivered a retrograde Canine Adenoviral Vector (CAV2) that encodes Cre-recombinase to the PAG (Hnasko *et al.*, 2006). CAV2 gains access to neurons primarily via their synaptic terminals (Soudais et al., 2001) before being transported retrogradely to the neuronal cell body leading to Cre expression. Thus Cre-dependent expression of actuator proteins will only occur in those PrL neurons that synapse in the PAG. Control animals had injection of Cre-dependent vectors to the cortex but no CAV-CMV-CRE to the PAG. Without Cre there should be no expression of actuator proteins allowing the evaluation of off target of effects of CNO (as well as identification of non-specific expression of actuators). Following expression of actuator

(n=24) and affective aspects (n=20) of pain like behaviour in neuropathic ($TNT^{PrL\text{-}P.ChR2\text{-}hM4Di}$ & $TNT^{PrL\text{-}P.Control}$) and uninjured ($Naive^{PrL\text{-}P.ChR2\text{-}hM4Di}$ & $Naive^{PrL\text{-}P.Control}$) rats. This investigation used a longitudinal design in which the contribution of PrL-P neurons to pain-like behaviour and nociceptive processing were assessed before and up to 42 days following peripheral nerve injury. Five neuropathic rats were then used in acute spinal electrophysiological experiments to assess effects of PrL-P neurons on nociceptive processing in the spinal dorsal horn.

Animals were assigned to experimental groups from different cages and selected at random but with no explicit randomization protocol. The experimenter was blinded to the experimental group and test substance. Some animals were removed from the analysed data sets due to:

- lack of or off target transfection (n=4/44)
- Incorrect placement of optic fibres outside the PrL (n=3/24)
- overt stress behaviour noted during experimental testing (n=3/44)
- incompatible laser stimulation parameters (1/24)
- incorrect dosing schedule in CPP paradigm (1/20)

Where appropriate, removal from one experimental protocol did not mean removal from the entire investigation as for example incorrect placement of an optic fibre did not preclude data from this rat being included for chemo-inhibition experiments which were not dependent on correct fibre placement.

Surgery

All surgery was conducted using sterile technique. Throughout procedures animals were kept hydrated and maintained at 37˚C using a thermostatically controlled heat mat. Post-surgery, all animals were monitored closely until wounds had healed, and the animal reached pre-surgery body weight.

Stereotaxic injection / implants

Animals underwent recovery surgery for the delivery of viral vectors to the PAG and mPFC, and implantation of optic fibres over the PrL. Rats were anesthetized with Ketamine (50mg.kg^{-1}; Zoetis, UK) / Medetomidine (0.3mg.kg^{-1}; Vetoquinol, UK), prepared for surgery and placed in a stereotaxic frame (Kopff, Germany). PrL-P projections extend bilaterally from each hemisphere with the ipsilateral projection bring denser that the contralateral projection (~60 v 40% of total labelled cells from retrograde tracing (Floyd *et al.*, 2000)). We targeted this denser ipsilateral projection and the targeting of left or right pathways was counterbalanced amongst animals.

We wanted to investigate cortical control of the DPMS that routes via the PAG. The ventrolateral column of the PAG is a known source of descending pain modulation (McMullan and Lumb, 2006a, 2006b) and it is the caudal section that receives ascending inputs from the lumbar spinal cord that represents the hind-paws (Mouton et al., 1997). In the rat, the caudal ventrolateral PAG (vlPAG) is primarily innervated from rostral portions of the PrL (Floyd et al., 2000). Therefore, we targeted delivery of CAV2-CMV-Cre to the caudal vlPAG and Cre-dependent AAV vectors to the rostral PrL on the same side.

A craniotomy was made over the PAG (AP: -7.5 to 8.5, ML: ±1.8 mm). CAV2-CMV-CRE (300nl / 4.95x10^{8} physical particles each site, Institut De Génétique Moléculaire De Montpellier, France) was delivered to the vlPAG at two caudal sites; AP -7.5, ML 1.8 and DV 5.4 and AP -8.00, ML 1.8 and DV 5.4mm from the brain surface with a 9˚ lateral to medial angle. Approximately 20nl of fluorescent microspheres (RetroBeads, Interchim, USA) were included in the injectant in some animals to mark the injection site.

A second craniotomy was made over mPFC (AP: +3.0 to 5.0, ML ±0.4-0.8) allowing injection of CRE-dependent AAVs encoding ChR2 and hM4Di :

- AAV2-EF1a-DIO-hChR2-EYFP (3.2 x 10^{12}vg/ml, UNC Vector Core, USA) &
- AAV2-hSyn-DIO-hM4Di-mCherry (4.6 x 10^{12} vg/ml, Addgene, USA)

These were mixed to equal titres and delivered to the rostral PrL at three anteroposterior locations and at two dorsoventral levels.

1. AP: +4.2, ML ±0.6, DV -2.5 & -2.0 mm
2. AP +3.8, ML ±0.6, DV -3.3 & -2.5 mm
3. AP +3.20, ML ±0.6, DV -3.3 & -2.5 mm

Viral vectors were delivered using a pulled glass pipette (Broomall, USA) attached via silicon tubing to a 25µl Hamilton syringe (Hamilton Company, USA). The whole system was filled with paraffin oil to allow for back filling of the pipette tip with viral vector. Delivery of the vector was controlled using a motorized syringe pump (Aladdin Syringe Pump, World Precision Instruments, USA), delivered at a rate of 200nl per minute and pipettes were left in place for ~10 minutes following vector delivery to allow for vector redistribution into the parenchyma.

An optic fibre (Lambda B, NA 0.66,length 4.4mm, width 200µm, light emitting length 2mm, Optogenix, Italy) was inserted to AP +4.2, ML ±0.6, DV -3.3mm from the cortical surface to enable light delivery across the full dorsoventral extent of the rostral PrL. Four skull screws were placed within separate cranial plates (M1, 1mm diameter, 3 mm length, NewStar Fastenings, UK). The optic fibre was secured to an adjacent scull screw using Gentamicin CMW DePuy bone cement (DuPuy Synthes, Johnson & Johnson, USA). The craniotomies from the vector injections were then filled with artificial dura (duraGel, Cambridge Neurotech, UK), the skull's surface covered with bone cement and the skin incision closed using adsorbable suture (Vicryl, Ethicon Inc, Johnson & Johnson, USA) leaving the optic fibre ferrule connector protruding.

Tibial Nerve Transection

Rats underwent recovery surgery for transection of the Tibial nerve (TNT) to produce a neuropathic pain state (Richardson *et al.*, 2015). This model was chosen for its gradual development of hypersensitivity as well as known contributions of descending pain modulatory system (Hughes *et al.*,

2013, 2015). Briefly, rats had induction of anaesthesia using isoflurane (5% in O_2; Henry Schinn, UK) and maintained at a surgical plane of anaesthesia using 2-3% isoflurane in O_2. The tibial nerve contralateral to the transfected PrL-P pathway was exposed and transected before the wound closed. An incision was made from below the hip, parallel to the femur and toward the knee. The underlying connective tissue was dissected away and the fascial plane between gluteus superficialis and bicep femoris was dissected to expose the branches of the sciatic nerve. The Tibial nerve was identified and carefully freed from connective tissue. Two ligatures of sterile 5.0 braided silk (Fine Science Tools, Germany) were tightly ligated approximately 5mm apart. The length of nerve between the two sutures was then transected and removed leaving the ligatures in place. The overlying muscle and skin were closed using adsorbable suture. Post-surgery no analgesic was provided so as to not interfere with pain state development.

Nociceptive Testing

Rats underwent longitudinal nociceptive sensory testing before and after TNT. This was conducted with / without opto-activation and chemo-inhibtion of PrL-P neurons to investigate their contribution to nociceptive threshold / pain-like behaviour in naïve and TNT rats. Neuropathic animals underwent testing for mechanical (Von Frey) before cold allodynia (acetone). There was more than 30 minutes between pre-CNO and post-CNO. All behaviour was recorded using a video camera (c930, Logitech, Switzerland) attached to a computer running video acquisition software (OBS Studio, Open Broadcaster Software) for offline analysis.

Heat Sensitivity: Thermal withdrawal latencies were measured for the hind-paw (Hargreaves *et al.*, 1988). Animals were habituated to the testing apparatus and experimenter for 10 minutes for at least 5 days prior to the start of the experiment. On experimental days animals were placed in a Plexiglass chamber, on top of a raised glass plate so that the infrared (IR) beam (Ugo Basile Plantar test, Italy) could be positioned under the plantar surface of the hind paws. The IR beam intensity was adjusted so that animals withdrew their paws at a latency of ~8s. Animals had IR light delivered to both left

and right hind paw with a ~4 min interstimulus interval between paws and hence >8 minute inter-stimulus interval between consecutive stimuli on the same paw to prevent sensitization. A cut off latency of 15 seconds was used to prevent tissue damage and subsequent sensitization. Stability of baseline withdrawal latency was considered to have been achieved when 3 consecutive latencies were within 2 seconds of each other.

Punctate mechanical sensitivity: To assess mechanical sensitivity animals were placed in a Plexiglass chamber on top of a raised metal grid to allow access to the plantar surface of the hind-paw. Rats were habituated to the testing apparatus and experimenter for 10 mins at least 5 days before the start of the experiment. Von Frey filaments (range 2.36-5.18mN) (Ugo Basile, Italy) were applied to the lateral aspect of the plantar surface of the hind-paw. The 50% withdrawal threshold was determined using the Massey-Dixon up-down method (Chaplan *et al.*, 1994)

Acetone: To assess cold sensitivity, rats were placed in a Plexiglass chamber on top of a raised metal grid to allow access to the plantar surface of the hind-paw. Using a 1ml syringe, a drop of Acetone (~0.1ml) was applied to the lateral aspect of the hind-paw and the number of nocicfensive events (paw shakes, licks and/or bites) recoded for up to 1 minute following application. This was repeated 3 times for each paw with an ISI of 2 minutes.

Manipulation of PrL-P Neurons.

For experiments involving opto-activation of PrL-P neurons Naïve$^{PrL\text{-}P.ChR2:hM4Di}$, Naïve$^{PrL\text{-}P.Control}$, TNT$^{PrL\text{-}P.ChR2:hM4Di}$ and TNT$^{PrL\text{-}P.Control}$ rats were tethered to a light source (445nm diode laser, Omicron Laserage, Germany) using an optical fibre patch cable (FT200EMT, Thor Labs, USA) to connect the head-mounted ferrule to the laser source allowing blue light to be delivered to the PrL via the implanted optic fibre. Once stable baseline withdrawal latencies were obtained two light stimulation rounds (445nm, 10-15mW, 20hz, 10ms pulse width, starting 1 minute before initiation of the IR beam) and two no light rounds were delivered to the PrL in a randomized order. Output of optic fibres were determined prior to implant by measuring the light power at the fibre tip over a range of laser strengths using a monitor

(PM120D, ThorLabs, USA). The average withdrawal latency for light stimulation rounds was compared to the average withdrawal latency for low-light stimulation rounds.

Experiments involving chemo-inhibition of PrL-P neurons were conducted on a separate day to opto-activation experiments. Once stable baseline withdrawal latencies for each hind paw were obtained animals received clozapine-N-oxide (CNO), the selective ligand for the hM4Di receptor, via an intraperitoneal injection at a dose of 2.5mg.kg^{-1}. Animals were placed back in the testing box and IR hind paw stimulation started 10 minutes after CNO delivery. Withdrawal latencies to plantar IR stimulation were recorded for both hind paws for at least 60 minutes post injection and the average withdrawal latency for recordings 20-40 minutes following CNO delivery were compared to the average baseline latencies for each paw.

The effect of chemo-inhibition of PrL-P neurons on mechanical withdrawal thresholds was assessed in TNT$^{PrL\text{-}P.ChR2\text{-}hM4Di}$ and TNT$^{PrL\text{-}P.Control}$ rats. Following, pre-CNO testing animals received systemic CNO (2.5mg.kg^{-1}) via an i.p injection and returned to their home cage. 20 minutes following CNO injection animals were placed back in the testing chamber and allowed to habituate for 10 minutes. Von Frey testing was repeated at 30 minutes post-CNO. The 50% withdrawal threshold obtained following CNO was compared to pre-CNO withdrawal threshold for that day.

The effect of opto-activation of PrL-P neurons on the 50% withdrawal thresholds was assessed in TNT$^{PrL\text{-}P.ChR2\text{-}hM4Di}$ and TNT$^{PrL\text{-}P.Control}$ rats at a late state (>21 days). Rats underwent baseline Von Frey testing prior to blue light delivery as previously described. Following, blue light (445nm, 10-15mW, 20hz, 10ms pulse width) was delivered continuously starting 1 minute prior to Von Frey testing and continuing to the end of testing. The 50% withdrawal threshold was compared with and without opto-activation of PrL-P neurons.

Behavioural Testing

Conditioned Place Aversion: A second cohort of TNT rats that did not have longitudinal sensory testing were tested in a conditioned place aversion paradigm to assess the contributions of PrL-P neurons to affective state. $TNT^{PrL\text{-}P.ChR2:hM4Di}$ and $TNT^{PrL\text{-}P.Control}$ rats were habituated to a three-compartment box with a neutral central compartment connecting two larger conditioning chambers. Chambers differed in their visual and tactile cues ('bars' or 'holes' for flooring and vertical or horizontal striped wallpaper with equal luminosity) to maximize their differentiation. A Baslar camera (acA1300-60 gm) with a varifocal lens (Computar H3Z4512CS-IR) connected to EthovisionXT (Noldus, NL) was used to record the time rats spent in each compartment. Rats were allowed to freely explore all three compartments for 20 minutes on day 1 to obtain baseline preference. No rats exhibited excessive chamber bias (>80% total time in a single chamber). After habituation, rats had TNT surgery and two days later started conditioning sessions (over 4 days) in which a compartment was paired with CNO (2.5mg.kg^{-1} i.p) or vehicle (2 sessions each). The chamber – drug pairings and the order in which they were presented were randomized and counterbalanced amongst animals. For each pairing session, rats received CNO or vehicle and were returned to their home cage for 10 minutes to prevent any negative association between restraint/injection and conditioning compartment. Rats were then placed in the conditioning compartment for 35 minutes. A single pairing session was conducted on each of the 4 days to prevent carry over of any CNO effects. Pairing sessions for each rat were conducted at the same time on each day. On the test day, animals were placed in the neutral compartment and allowed to freely explore all three compartments for a total of 20 minutes and the time spent in each compartment recorded. A 'preference score' was calculated by taking the percentage of time spent in the CNO-paired compartment on test day (relative to the total time spent in all three chambers), normalized by the percentage time spent in the same chamber on pre-test day (relative to total time spent in all three chambers) (Meda et al., 2019). Preference scores for CNO and Vehicle paired chambers were compared within each animal. Preference or aversion to CNO-paired chamber is expected to be influenced by the valence of chemo-inhibition of PrL-P neurons. Preference scores of < 1 indicate place aversion and those > 1 preference.

Electrophysiology

In vivo spinal dorsal horn recordings: $TNT^{PrL\text{-}P.ChR2:hM4Di}$ rats were terminally anaesthetised with urethane (1.2-2g/kg i.p, Sigma). The spinal cord was exposed by laminectomy over T13-L3 spinal segments to allow access to the spinal cord (Leith *et al.*, 2014; Drake *et al.*, 2016).The animal was placed in a stereotaxic frame with spinal clamps (Narishige Japan) and the spinal cord stabilised at T12 and L4, and a bath formed by skin elevation. A reference electrode was placed in nearby musculature. The spinal dura matter was carefully removed using bent tipped needles (25G) under binocular vision. The skin pool was filled with warm agar and, once cool, a recording window cut out and the void filled with warm (~37^{o}C) mineral oil. Using a hydraulic manipulator (Narishige, Japan) a 4 contact silicon probe (Q-probe, NeuroNexus, USA) was advanced into the spinal dorsal horn and recordings of single dorsal horn neurones made between 250 – 800µm deep to the surface. Neural activity was amplified and digitised on a headstage microchip (RHD2132, Intan technology) and captured to computer at 30kHz using an Open Ephys acquisition system and associated software (OpenEphys, USA).

Low threshold brush and touch applied to the paw were used as a search stimulus as the recording electrode was advanced into the spinal dorsal horn. Once single units were isolated non-noxious and/or noxious mechanical (VonFrey filaments) and cold (acetone) were applied to the receptive field on the lateral aspect of the hind leg/paw. Wide dynamic range neurones were identified by their graded response to non-noxious and noxious stimuli (≥15g Von Frey). A baseline stimulus – response relationship was obtained by applying 4 and 15g von Frey filaments and a single drop of acetone to the receptive field. This was repeated 3 times for each stimulus with a 10s inter-stimulus interval between Von Frey filaments and 1 min between acetone drops. To optogenetically activate the PrL-P neurons, blue light was delivered via the implanted optic fibre (445nm, 10-15mW, 20Hz, 10ms pulse width) continuously starting 1 min prior to peripheral stimulation and lasting until the end of the stimulus set (4 & 15g vF hairs and acetone stimuli were reapplied 3 times). The average number of

evoked action potentials for each stimulus was compared before, during and 5 mins following opto-activation of PrL-P neurons.

Histological Processing

Tissue collection and processing: Rats were killed with an overdose of pentobarbital (20mg/100g, i.p, Euthalal, Merial Animal Health) and perfused trans-cardially with 0.9% NaCl (1ml per gram) followed by 4% formaldehyde in phosphate buffer (PB). The brains were dissected out and post-fixed overnight in the same solution before cryoprotection in 30% sucrose in PB. Coronal sections were cut at 40µm using a freezing microtome and left free floating for fluorescent immunohistochemistry or mounted on slides to identify optic fibre tracts and/or injection sites for viral vector delivery using light microscopy.

Immunofluorescence: Tissue sections were incubated free floating on a shaking platform with phosphate buffer containing 0.3% Triton-X100, 5% normal goat serum (Sigma) and primary antibodies to detect EGFP (ab13970, Abcam) or mCherry (5993-100, BioVision) for 24 hours at room temperature. After washing with PB, sections were incubated for 3 hours at room temperature with an appropriate Alexa Fluor secondary antibody. Following, sections were washed before mounting on glass slides in 1% gelatin solution and, once dried, cover slipped using FluroSave reagent (345789, Merck-Millipore, Germany). Sections were imaged on a Leica DM16000 inverted epifluorescence microscope equipped with Leica DFC365FX digital camera and LAS-X acquisition software.

Transduction Mapping: To create maps of the distribution of transfected neurons within the mPFC, a series of coronal mPFC sections from 3 animals were manually plotted. Each section was paired to a matching coronal diagram from the Rat Brain Atlas (Paxinos and Watson, 2007), at ~120µm intervals (every third section). Using an epiflurescent microscope (Zeiss Axioskop II inverted microscope equipped with a CooLED pE-100 excitation system, filter blocks - red: filter set number 15 (DM 580 nm, BP 546/12 nm, LP 590 nm) and green: filter set number 09 (DM 510 nm, BP 450–490 nm, LP 515 nm), mCherry+ cells were plotted. The diagrams were digitised into the photo editing software GIMP.2

(Creative Commons) allowing superimposition to create conjunction maps indicating the extent of labelled areas of the mPFC within each cohort. A digital grid was used to divide up the cortical field and the number of positively labelled neurones counted within each 0.2mm^2 grid from each animal. The consistency of positive labelled neurons within each grid square was represented on a grayscale with black indicating positively labelled cells in all rats and white indicating no cells. To determine the proportion of transfected neurons that co-expressed both ChR2-EYFP and hM4Di-mCherry composite widefield images were taken at 20X magnification of every 6th section in a series of consecutive mPFC section from ~+5.10 to +2.8 mm from bregma and from three experimental animals. From these images the distribution of EYFP, mCherry, and co-localised neurons were quantified.

Drugs

ClozepineN-Oxide (Tocris, UK) was purchased and made up on the day of use in DMSO and diluted with 0.9% NaCl to a final concentration of 2.5mg.ml^{-1} and 5% DMSO.

Quantification and Statistics

All statistical analysis was conducted using GraphPad Prism 8. All data are presented as mean ± SEM. Sample sizes were estimated from previous experience and with reference to literature (Hughes *et al.*, 2013; Drake *et al.*, 2016; Hirschberg *et al.*, 2017). Students t-test (paired and unpaired), repeated measures two way ANOVA or Mixed Model were used to compare groups as appropriate. This mixed model uses a compound symmetry covariance matrix and is fit using Restricted Maximum Likelihood (REML). Sidak's or Dunnett's post-test were used for comparisons between multiple groups and where appropriate. The number of replications (n) is the number of data points used in the statistical test that is either the number of animals for behavioural testing or the number of neurons for electrophysiological experiments.

Results

Targeting mPFC → PAG neurons in the pre-limbic cortex.

To make selective manipulations of medial prefrontal cortex (mPFC) neurons that project to the PAG we expressed the excitatory light activated ion channel, Channelrhodopsin2 (ChR2) and the inhibitory ligand gated g-protein coupled receptor, hM4Di, in mPFC pyramidal neurons using an intersectional and Cre-dependent approach (Fig 1A). This approach led to the expression of hM4Di-mCherry and/or Chr2-YFP on average in 248±71 mPFC pyramidal neurons (n=3 rats) that were located in layer 5/6 (Fig1 B,C). Colocalization of hM4Di-mCherry and Chr2-EYFP was found in 76.1±3.3% of labelled neurons with 23.9±3.3% expressing hM4Di only and no cells that expressed ChR2-EYFP alone. The majority of labelled neurones were found in the pre-limbic cortex (PrL versus Medial Orbital 72±1.5 vs 10.8±4.6%) (Fig1 D&E). Successful targeting of the PrL-P neurons was confirmed by the presence of hM4Di-mCherry and Chr2-EYFP labelled fibres within the ventrolateral (vl)PAG (Fig 1F). In control animals, in which no CAV-CMV-CRE was delivered to the vlPAG there was negligible expression of actuator protein in the mPFC after delivery of cre-dependent AAV vectors (Sup Fig1).

PrL-P neurons bidirectionally regulate nociception in naïve rats.

To determine the effect of PrL-P neurons on noxious withdrawal threshold in healthy animals, ChR2/hM4Di-expressing (Naïve$^{PrL\text{-}P.ChR2:hM4Di}$) and control (Naïve$^{PrL\text{-}P.Control}$) rats underwent Hargreaves' testing with opto-activation or chemo-inhibition of PrL-P neurons (Fig 2A-F). Opto-activation of PrL-P neurons (10-15mW, 20Hz, 10ms pulse) in Naïve$^{PrL\text{-}P.ChR2\text{-}hM4Di}$ rats produced a significant increase in thermal withdrawal latencies ipsilateral, but not contralateral, to the transfected PrL-P pathway (baseline versus PrL-P opto-activation = 7.5±0.4 vs 10.4±0.9 seconds, p=0.008, paired t-test, n=10) (Fig 2 B & C). The equivalent illumination paradigm in Naïve$^{PrL\text{-}P.Control}$ rats did not alter ipsilateral or contralateral withdrawal latencies (Fig 2B,C&D). Conversely, chemo-inhibition (2.5mg.kg-1 CNO i.p.) of PrL-P neurons in the same Naïve$^{PrL\text{-}P.ChR2\text{-}hM4Di}$ rats that received opto-activation significantly decreased the average withdrawal ipsilateral, but not contralateral, to the transfected PrL-P pathway

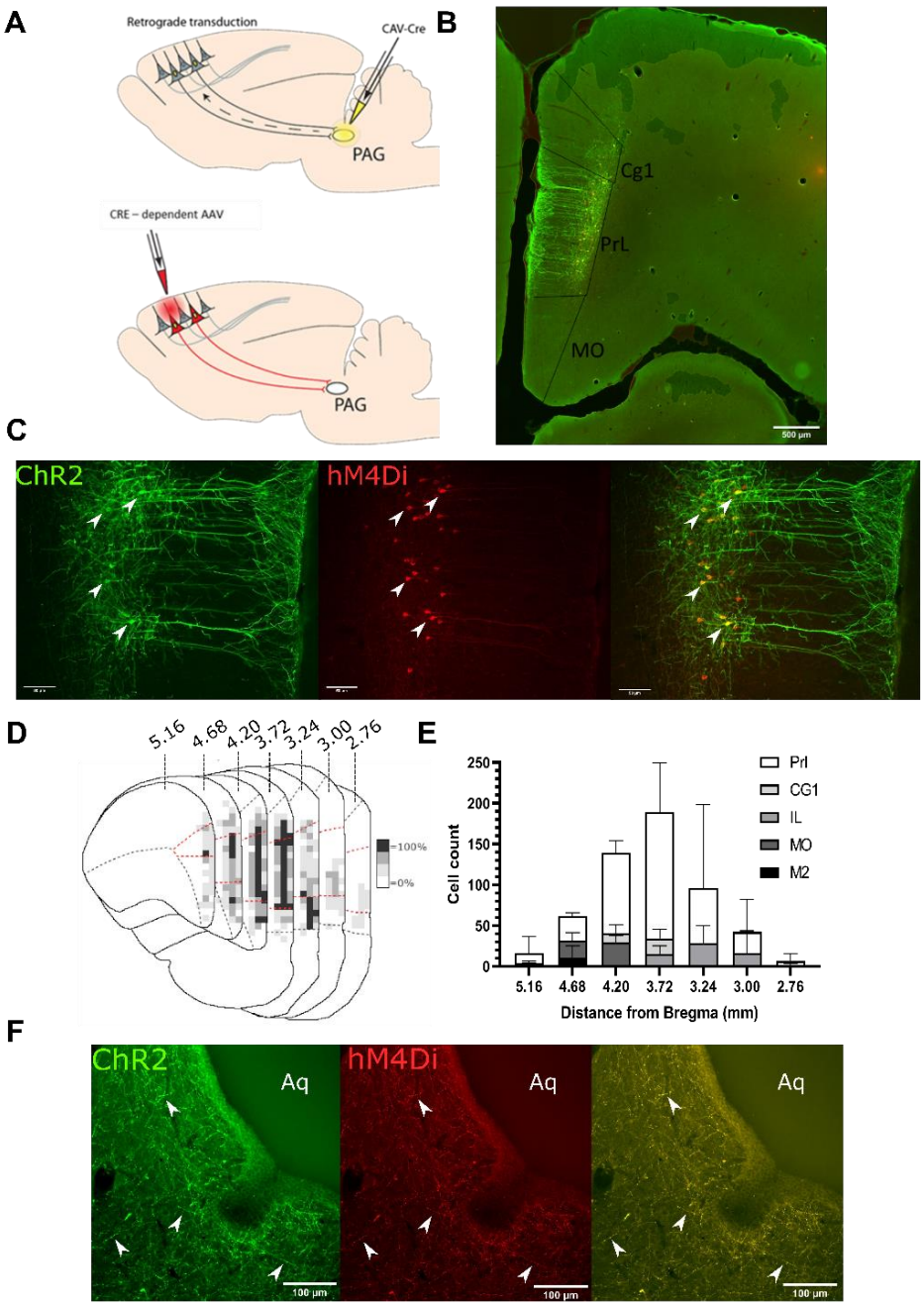

Figure 1. Transfected mPFC→PAG neurons arise mainly from the pre-limbic cortex. A - Intersectional viral vector strategy using retrograde canine adenovirus and Cre-dependent adeno-associated viral vectors to express genetically encoded actuators (both ChR2 and hMD4i) to target mPFC neurons that project to the PAG. **B** – Photomicrograph of mPFC showing labelled neurones residing mainly in the pre-limbic cortex. **C** – Pre-limbic cortex with co-localisation of mCherry (hM4Di) and EYFP (ChR2) in neurons projecting to PAG (many examples but several marked with white arrows). **D** – Conjunction plot illustrating location of mPFC→PAG neurons throughout the medial prefrontal cortex (n=3 rats). Darker shading indicates positional overlap of positively labelled (hM4Di) neurons from more than one animal (light = 1 animal, mid = 2, dark =3). Dotted red line demarks the pre-limbic cortex. **E** - Comparative distribution of mPFC→PAG neurons throughout the cortex (mean ± SEM). **F** – Photomicrograph showing ChR2-EYFP & hM4Di-mCherry containing fibres from mPFC projecting to the ventrolateral region of PAG (many examples but several marked with white arrows).

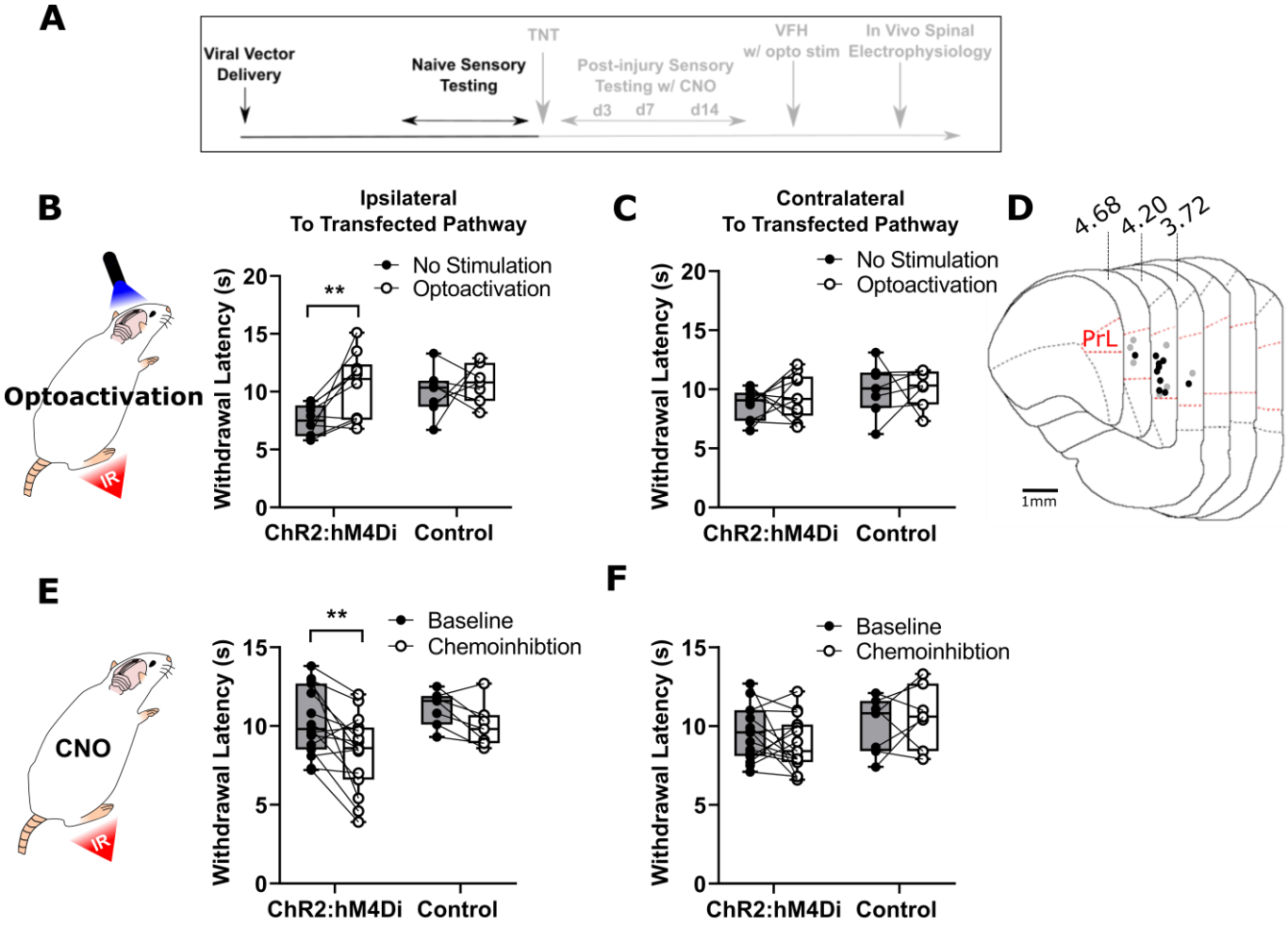

Figure 2. PrL-P neurons bidirectionally regulate nociception in naive rats. A – Experimental timeline. B – Illumination of PrL (445nm, 20Hz, 10-15mW, 10ms pulse, concomitant with hind-paw heating) in Naive$^{PrL.ChR2:hM4Di}$ rats increases thermal withdrawal latencies on the ipsilateral hind paw but not in Naive$^{PrL.Control}$ rats that do not express ChR2 (Paired t-test p=0.008, n=10 for ChR2:hM4Di group; p=0.55 n=7 for control group) and **C –** Equivalent illumination of PrL has no effect on the thermal withdrawal latency in the contralateral hind-paw in either Naive$^{PrL.ChR2:hM4Di}$ or Naive$^{PrL.Control}$ (paired t-test p=0.40, n=10 for Naive$^{PrL.ChR2:hM4Di}$ rats; p=0.90, n=7 for the Naive$^{PrL.Control}$ rats). **D** – Optic fibre tip locations in the mPFC from Naive$^{PrL.ChR2:hM4Di}$ (●) and Naive$^{PrL.Control}$ (○) rats. For simplicity, fibre placements are depicted in a single hemisphere. **E** – CNO (2.5mg.kg^{-1} i.p) in Naive$^{PrL.ChR2:hM4Di}$ rats decreased withdrawal latencies (mean value at 20-40mins post injection) on the ipsilateral paw but not in Naive$^{PrL.Control}$ rats (Paired t-test p = 0.006, n = 15 for Naive$^{PrL.ChR2:hM4Di}$ rats; p=0.55, n = 7 for Naive$^{PrL.Control}$ rats) and **G –**CNO had no effect on the thermal withdrawal latency of the contralateral hind-paw in either Naive$^{PrL.ChR2:hM4Di}$ rats or Naive$^{PrL.Control}$ rats (paired t-test p=0.24 n=15 for Naive$^{PrL.ChR2:hM4Di}$ rats; p=0.68, n=7 for Naive$^{PrL.Control}$ rats).

(Baseline vs chemo-inhibition of PrL-P = 10.3±0.6 vs 8.3±0.6 seconds, p=0.006, paired t-test, n = 15 (Fig 2 E&F)). CNO had no significant effect on withdrawal thresholds in Naïve$^{PrL\text{-}P.ChR2\text{-}hM4Di}$ rats (Fig

2E&F). These findings demonstrate that there is a tonic level of activity within the PrL-P pathway that dynamically regulates nociception in the absence of any process of sensitisation.

Tonic activity in PrL-P neurons delays the development of neuropathic hypersensitivity.

The TNT model of neuropathic pain was used to assess the contribution of PrL-P neurons to the development of sensitisation (Fig 3A-D). $TNT^{PrL\text{-}P.ChR2\text{-}hM4Di}$ and $TNT^{PrL\text{-}P.Control}$ rats had nociceptive sensory testing before and after CNO (2.5mg.kg^{-1}, imp Fig 3C) longitudinally up to 42 days post-nerve injury (suppl Fig 2). Chemo-inhibition of PrL-P neurons unmasked mechanical and cold hypersensitivity In $TNT^{PrL\text{-}P.ChR2\text{-}h\ M4Di}$ rats, for the ipsilateral, nerve injured, hind paw at day three post nerve injury (Fig 3 E&I). The mechanical withdrawal threshold (von Frey) was reduced no average by 80% on day 3 post TNT, from 6.0±1.3g (pre-CNO) to 1.2±0.5g (post-CNO) (2Way ANOVA. CNO $F(1,30)=20.09$ $p=0.0001$. Sidak's post-test day 3 pre-CNO vs CNO $p=0.008$, n=16) (Fig 3E). Similarly, the number of cold-evoked nocicifensive behaviours (foot flicking, biting and grooming) was significantly increased ipsilaterally by PrL-P chemo-inhibition at day 3 post-TNT from 2.8±0.5 to 5.8± 0.7 events (2Way ANOVA. CNO $F(1,30)=9.6$ $p=0.004$, Sidak's post-test day 3 pre-CNO vs Post CNO $p=0.003$, n=16) (Fig 3I). At 7 days post nerve injury, PrL-P chemo-inhibition also significantly decreased the ipsilateral mechanical withdrawal threshold from 2.5±0.5 to 0.30±0.06 grams (Sidaks post-test $p=0.001$, n=16, Fig 3E). For the contralateral (uninjured) paw PrL-P chemo-inhibition significantly reduced mechanical withdrawal thresholds at day 3 post-TNT from 13.5±0.7 to 9.0±1.4 grams (2Way ANOVA. CNO $F(1,30) = 5.77$ $p=0.02$, Sidak's post-test day 3 pre-CNO vs CNO $p=0.03$, n=16) but not thereafter (Fig3 F). From 14 days post-nerve injury and up to 42 days PrL-P chemo-inhibition ceased to significantly change either mechanical or cold-evoked nocifensive behaviour on the ipsilateral hind-paw (Fig3 E&I, Supl Fig 2). In

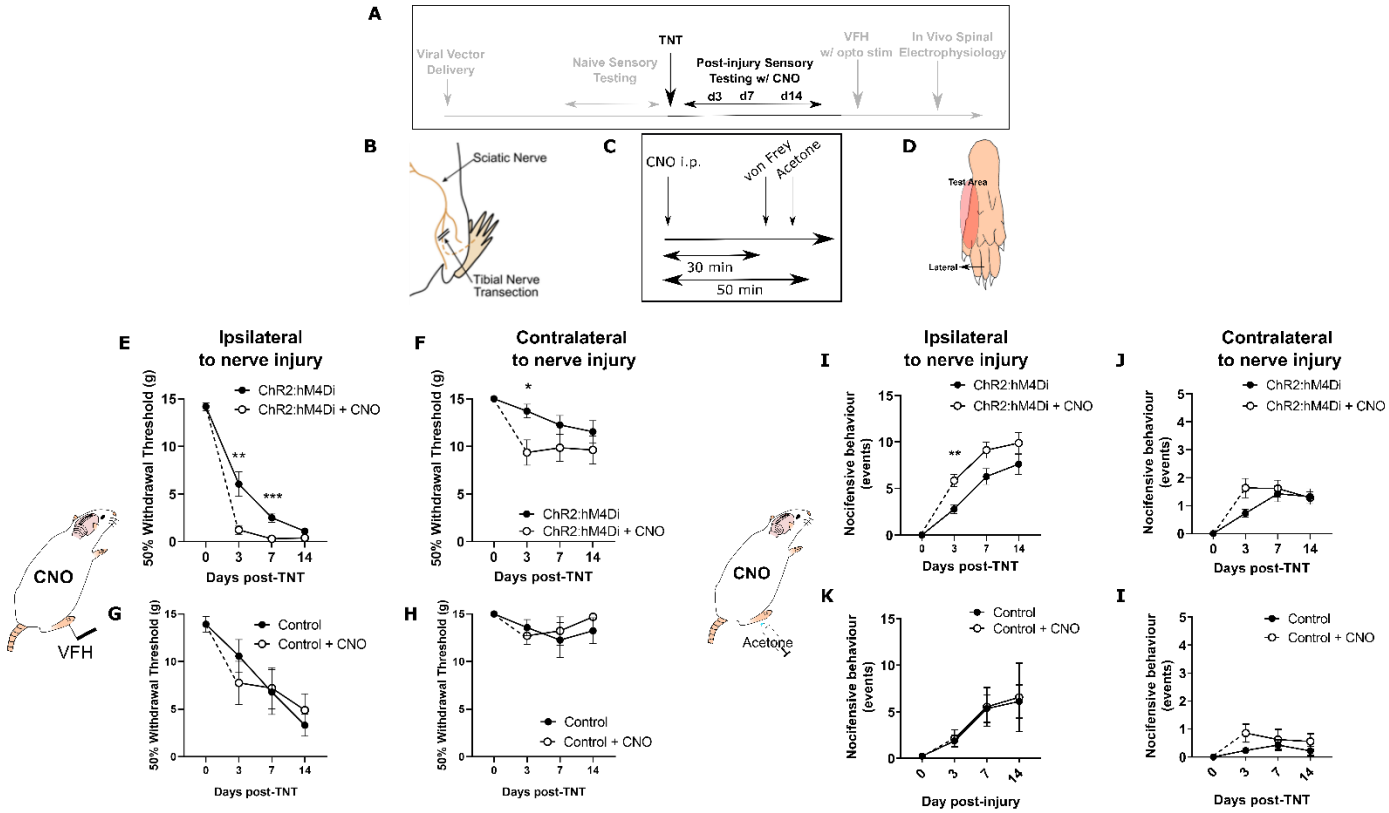

Figure 3. Inhibition of PrL-P neurons unmasks hypersensitivity in neuropathic rats. A – Experimental timeline. **B** –Tibial nerve transection (TNT) was used to produce the neuropathic injury. **C**- Sensory testing was conducted at 30 mins after systemic delivery of CNO and **D-** testing was conducted on the lateral plantar surface of the hind-paw in a receptive field adjacent to injured tibial nerve. **E** – In $TNT^{PrL.ChR2:hM4Di}$ rats, CNO (2.5mg.kg^{-1} i.p) reduces mechanical withdrawal threshold at 3 and 7 days post nerve injury on the ipsilateral (injured) hind-paw (2-way ANOVA, Main effect CNO F(1,30)=20.09 p=0.0001, Time x CNO F(2, 60)=6.892 p=0.002. Sidaks post-test **p<0.01, ***p<0.001, n= 16) and **F -** on the contralateral paw at 3 days post-injury (2Way ANOVA, CNO F(1,30) = 5.77 p=0.02, Sidak's post-test *P<0.05, n = 16). **G & H** - In $TNT^{PrL.Control}$ rats, the same dose of CNO did not alter mechanical withdrawal thresholds on either the ipsilateral or contralateral hind-paw (2-way ANOVA, main effect; ipsilateral CNO F(1,14)=0.02 p=0.90, n=8 & contralateral CNO F(1,14)=0.15 p=0.71, n=8 respectively). **I** – In $TNT^{PrL.ChR2:hM4Di}$ rats, CNO increased acetone-evoked nocifensive events at 3 days post injury on the ipsilateral paw (2-way ANOVA, main effect CNO F(1,30)=9.6 p=0.004, Sidak's post-test **p<0.001, n=16) but not contralaterally (**J** – 2WAY ANOVA, main effect CNO F(1,29)=1.3 p=0.26, n=16). **K&I -** In $TNT^{PrL.Control}$ rats, CNO did not alter acetone evoked nocicfensive behaviour (2-way ANOVA, main effect CNO ipsilateral F(1,12)=0.02, p=0.89, n=7 **;** main effect CNO contralateral F(1,12)=2.2 p=0.16, n=7).

TNT$^{PrL\text{-}P.Control}$ rats, CNO failed to significantly change either mechanical withdrawal thresholds or cold (acetone) evoked nocicfensive behaviour on either the ipsilateral or contralateral paw at any timepoint post-TNT (Fig 3G,H, K, I). These results suggest that PrL-P neurons provide a tonic descending drive to oppose peripheral sensitisation during the early stages of development of neuropathic pain but this effect is lost as sensitisation becomes established after 14 days.

Chemogenetic inhibition of PrL-P neuronal activity is aversive in TNT rats with latent sensitisation.

Neuropathic sensitisation is associated with negative affect (King *et al.*, 2009; Hirschberg *et al.*, 2017) which raises the possibility that PrL-P neurons act to oppose the development of negative affect. If so, then chemo-inhibition of PrL-P neurons in the early phase after nerve injury would be expected to cause aversion. To test this proposition, TNT $^{PrL\text{-}P.ChR2\text{-}hM4Di}$ and TNT$^{PrL\text{-}P.Control}$ rats had place aversion testing with CNO conditioning between days 2 and 5 post-TNT (Fig 4A). TNT $^{PrL\text{-}P.ChR2\text{-}hM4Di}$ animals showed an aversion to the CNO paired chamber (post-conditioning – pre-conditioning time = -82.9±24.7 seconds, n=8) (Fig 4B&C). We calculated the preference of each rat for the CNO or vehicle paired chamber and found TNT $^{PrL\text{-}P.ChR2\text{-}hM4Di}$ animals showed a significantly reduced preference score compared to the vehicle paired chamber (Fig 4C; CNO paired vs vehicle paired = 0.8±0.04 vs 1.06±0.06, paired t-test p=0.04, n=8). TNT$^{PrL\text{-}P.Control}$ animals showed no difference in preference score for CNO and vehicle paired chambers (Fig 4D, CNO paired vs vehicle paired = 1.1±0.18 vs 1.00±0.21, paired t-test p=0.81, n=9). These findings are consistent with PrL-P neuronal activity opposing the development of negative affect in the immediate period after nerve injury

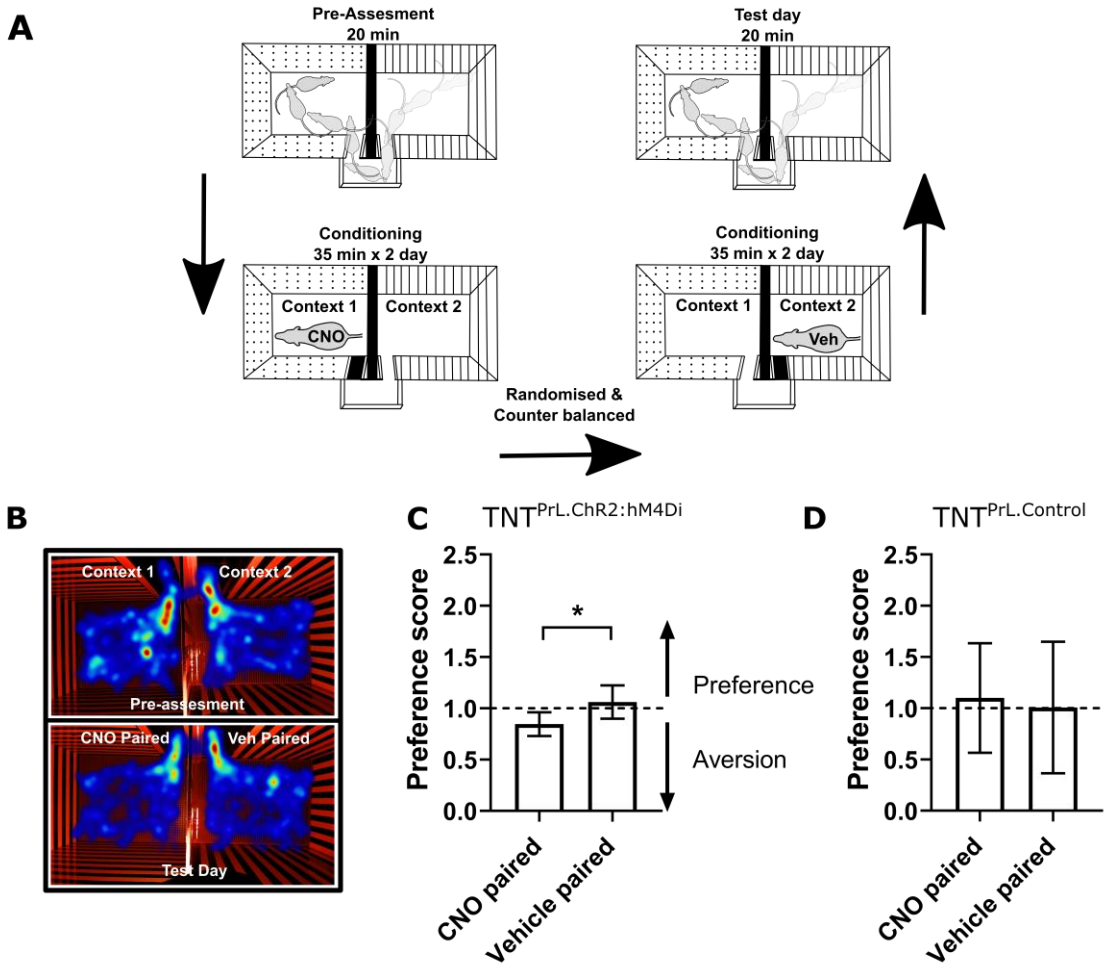

Figure 4. Inhibition of PrL-P neurons produces aversion in neuropathic animals. A –conditioned place aversion protocol. **B**– Example heatmap visualisation of the time spent within the testing chambers prior (top) and following conditioning with CNO or vehicle. **C** – Group data showing conditioning with CNO in $TNT^{PrL.ChR2:hM4Di}$ rats 2-5 days after TNT produced aversion (paired t-test, p=0.04, n=8). **E** – CNO administration to $TNT^{PrL.Control}$ rats did not produce aversion (Paired t-test, p=0.81, n=9

Restoration of PrL-P neuronal tone is analgesic in established neuropathic sensitisation.

To test whether the loss of function by PrL-P neurons in later stage neuropathic sensitisation could be reversed we employed opto-activation of PrL-P to test if it was still able to suppress sensitisation (Fig 5). Opto-activation in $TNT^{PrL\text{-}P.ChR2:hM4Di}$ rats (20Hz, 10ms, 10-15mW) produced an increase in the

mechanical withdrawal threshold (Baseline vs opto-activation vs recovery = 1.7±0.5 vs 5.2±1.4 vs 2.1±0.5 grams, 1Way RM ANOVA, p=0.02, Sidak's post-test baseline vs opto-activation p=0.01, n = 9) (Fig 5B). Equivalent illumination in $TNT^{PrL\text{-}P.control}$ rats did not change the mechanical withdrawal threshold (baseline vs opto-activation vs recovery = 1.4±0.5 vs 1.0±0.4 vs 1.4±0.3, n=3) (Fig 5B). This data indicates that the PrL-P neurons are still capable of supressing neuropathic sensitisation in late stage TNT rats.

PrL-P produces analgesia in neuropathic pain by inhibition of dorsal horn nociceptive responses.

To better understand the mechanism by which the PrL-P neurons suppress neuropathic sensitisation, $TNT^{PrL\text{-}P.ChR2:hM4Di}$ rats were tested in acute spinal electrophysiology experiments. Opto-activation of PrL-P neurons attenuated the evoked responses of spinal dorsal horn wide dynamic range (WDR) neurons (Fig 5C-F). The number of action potentials evoked by a punctate mechanical stimulus with a 4g and 15g Von Frey hair was reduced on average by 43% and 23% respectively (Fig 5D&E. 4g vF, baseline vs opto-activation vs recovery = 25.7±5.0 vs 14.63±3.1vs 25.0±45.0 action potentials. Mixed Model (REML), Fixed effect Treatment p=0.007. Dunnett's post-test baseline versus opto-activation p=0.009, n=9; Fig 5E, 15g vF, baseline vs opto-activation vs recovery = 45.17±6.9 vs 34.5±6.9 vs 43.9 ±7.8. Mixed Model (REML) p=0.10, Dunnett's post-test baseline versus opto-activation p=0.04, n=9). Similarly, cold-evoked spinal WDR neuron activity was significantly reduced by opto-activation of PrL-P neurons (Fig 5F, average reduction of 47%, Baseline vs opto-activation = 172.0±38.8 vs 91.7±42.2 action potentials, paired t-test, p=0.04, n=4). This data indicates that the PrL-P neurons are acting to suppress neuropathic sensitisation (punctate and cold allodynia) at a spinal level through the engagement of the DPMS.

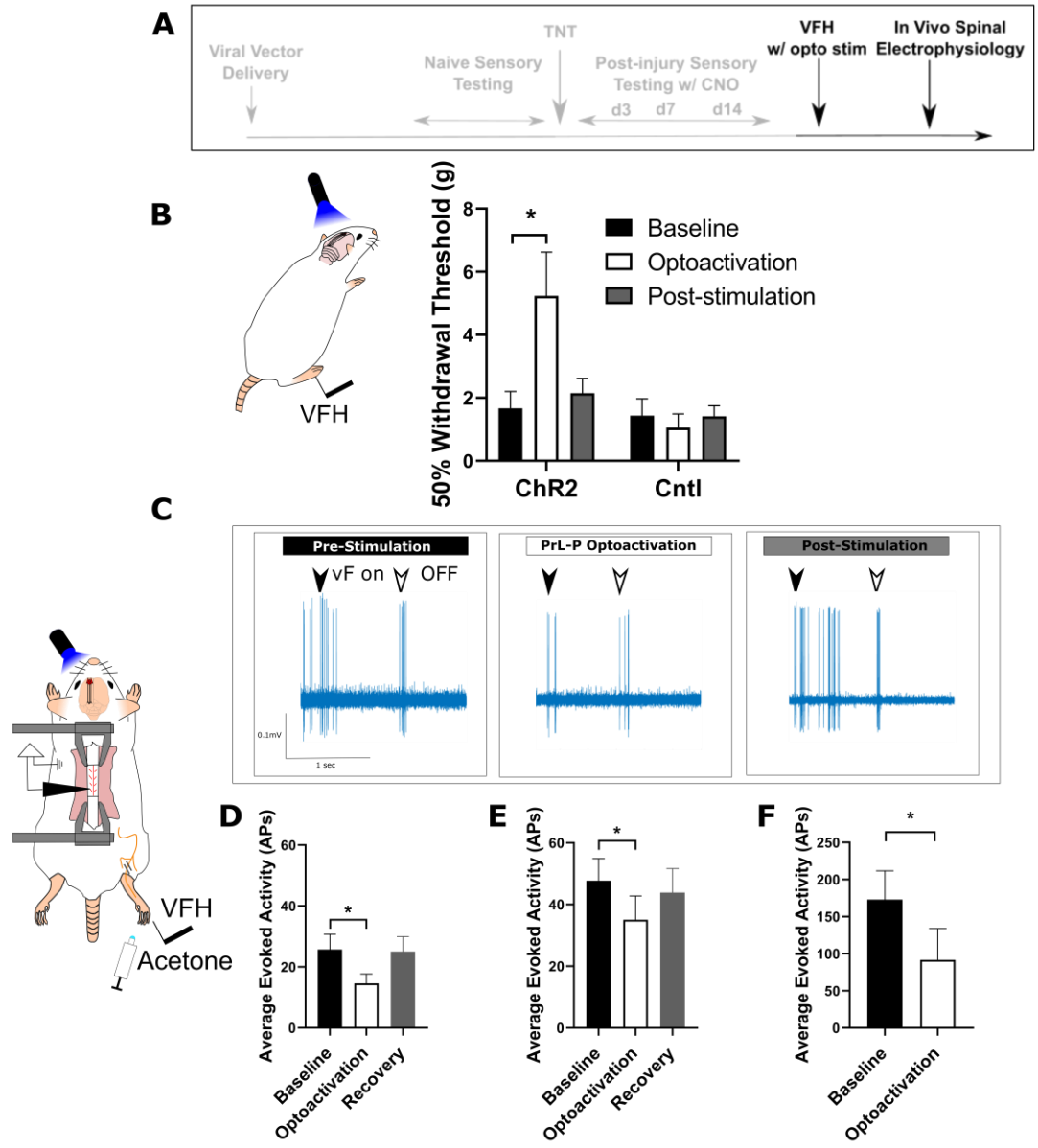

Figure 5. Activation of PrL-P neurons produces analgesia in neuropathic rats by inhibition at a spinal level. A – Experimental timeline. **B** – Delivery of blue light (445nm, 20Hz, 10-15mW, 10ms pulse, concomitant with hind-paw stimulation) produced a significant increase in mechanical withdrawal thresholds in $TNT^{PrL.ChR2:hM4Di}$ rats (RM ANOVA, Treatment F(1.12, 8.96)=8.07 p=0.02, Sidak's post-test *p<0.05, n=9) but not $TNT^{PrL.Control}$ (RM ANOVA, Treatment F(1, 2)=0.35 p=0.61, n=3). **C** – Example raw data trace illustrating suppression of von Frey hair evoked spinal dorsal horn neuron activity during blue light (420nm, 10-15mW, 10ms duration, concomitant with hind-paw stimulation) delivery to the PrL in $TNT^{PrL.ChR2:hM4Di}$ rats (arrows demark beginning and end of stimulus). **D** – Group data illustrating significant suppression of 4g evoked spinal dorsal horn neuronal activity by illumination of the PrL in $TNT^{PrL.ChR2:hM4Di}$ rats (Mixed Model (REML), p=0.007, Dunnet's post-test *p<0.05, n=10). **E** – Illumination of the PrL in $TNT^{PrL.ChR2:hM4Di}$ rats also significantly supressed 15g evoked spinal dorsal horn neuronal activity (Mixed model (REML), p=0.10, Dunnet's post-test *p<0.05, n=10.) **F** – Delivery of blue light to the Prl In $TNT^{PrL.ChR2:hM4Di}$ rats significantly decreased acetone evoked spinal dorsal horn neuronal activity (paired t-test, p=0.04, n=4

Discussion

By using a longitudinal study design, we have been able to reveal the dynamic contributions of pre-limbic to periaqueductal grey communication to neuropathic pain state development. In uninjured animals, we found PrL-P neurons to exert tonic inhibitory control over evoked noxious withdrawal responses suggesting they were involved with the moment to moment regulation of nocifensive behaviour. Following tibial nerve injury, rats developed mechanical and thermal allodynia that plateaued at around 14 days post injury. Chemo-inhibition of PrL-P neurons at 3- and 7-days post-injury revealed latent hypersensitivity both ipsilateral and contralateral (day 3 only) to nerve injury and produced place aversion in a conditioned place preference paradigm. However, chemo-inhibition of PrL-P neurons at more than 14 days post-injury failed to significantly affect mechanically or thermally evoked pain-like behaviour. These findings are consistent with there being a tonic activity in PrL-P neurons that suppresses hypersensitivity early after nerve ligation but this is lost with time as the neuropathic pain phenotype emerges. Despite the loss in function, opto-activation of PrL-P neurons during later stages of neuropathic pain produces anti-allodynic effects in neuropathic animals achieved, at least in part, by inhibitory effects on spinal nociceptive processing. We suggest that this cortical – midbrain – spinal network allows executive control of nociception and regulation of pain and that it is the loss of cortical drive to the descending pain modulatory system that underpins the expression of neuropathic sensitisation after nerve injury.

Loss of endogenous inhibitory control of CNS pain processing (Staud, 2013) and altered functional connectivity between the mPFC and the PAG is a shared feature of a wide variety of human chronic pain conditions (Jensen *et al.*, 2012; Yu *et al.*, 2014; Chen *et al.*, 2017; Segerdahl *et al.*, 2018) – our findings suggest these changes are causally related. The human mPFC, including the anterior cingulate cortex (ACC), is increasingly recognised as a key locus in the development and maintenance of chronic pain, with changes in structure and function that are associated with, and sometimes predictive of, the transition to chronic pain (Apkarian *et al.*, 2004; Baliki *et al.*, 2012; Hashmi *et al.*, 2013; Baliki and

Apkarian, 2015). The PAG is a key node in the DPMS but also an important orchestrator of autonomic and sensorimotor systems that is engaged to support mPFC function in aversive learning, emotional modulation and pain modulation which are all relevant to the chronic pain phenotype (Keay and Bandler, 2001; Franklin *et al.*, 2017; Rozeske *et al.*, 2018; Huang *et al.*, 2019). In humans, changes in functional connectivity between the mPFC/ACC, and the PAG are commonly observed in experimental paradigms that produce emotional, attentional and placebo/nocebo influences on pain as well following delivery of analgesic drugs and often interpreted as reflecting engagement of the DPMS (Wager *et al.*, 2004; Wiech *et al.*, 2014; Wanigasekera *et al.*, 2018; Oliva *et al.*, 2020). Moreover, changes in the functional connectivity between regions of the mPFC and the PAG are often correlated with changes in pain perception and/or disease progression, (Cifre *et al.*, 2012; Hemington and Coulombe, 2015; Harper *et al.*, 2018; Segerdahl *et al.*, 2018; Wanigasekera *et al.*, 2018; González-Roldán *et al.*, 2020). Here we provide evidence in rodents that the PrL, a component of the rodent mPFC, can engage the DPMS to affect nociception and loss in PrL-P neuron function is causally related to the development of the neuropathic pain state in rats. We suggest that changes in functional communication between the mPFC and the PAG, whether trait, age or disease related, likely manifest as alterations in the descending control of spinal nociception.

Pre-clinical findings suggest that loss of mPFC – PAG functional communication is explained by both local and inter-regional network alterations. In neuropathic rodents, at 7-10 days post-nerve injury, there is a decline in spontaneous and evoked PrL layer 5 pyramidal cell activity including those that project to the PAG (Cheriyan and Sheets, 2018; Mitrić *et al.*, 2019). This reduction in PrL projection neurones excitability is produced by enhanced feedforward inhibition from local GABAergic interneurons, and driven by inputs from the basolateral amygdala (Zhang *et al.*, 2015; Cheriyan *et al.*, 2016; Kiritoshi, Ji and Neugebauer, 2016; Cheriyan and Sheets, 2018; Huang *et al.*, 2019). Opto-inhibition of BLA inputs to the PrL releases PrL-P neurons to engage descending inhibitory control from the PAG (Huang *et al.*, 2019). PrL-P neurons are glutamatergic and target both GABAergic and glutamatergic neurones in the PAG (Franklin *et al.*, 2017; Huang *et al.*, 2019) but engage descending

inhibitory control from the PAG that is associated with release of local GABAergic control (Tovote *et al.*, 2016; Huang *et al.*, 2019). We suggest that the BLA – PrL – PAG – spinal network is central to the expression of neuropathic pain and therapeutics that reengage cortical control of descending pain modulation may be effective in treating both sensory and affective disturbances in chronic pain. However, whilst BLA inputs to the PrL drive sensory hypersensitivity and negative affect by reducing descending inhibition of the spinal dorsal horn, BLA inputs to the dorsal cingulate regions mitigate pain related aversion (Meda *et al.*, 2019). Additionally, in neuropathic rodents, the E/I ratio of BLA inputs into infralimbic projections to the PAG remain unchanged (Cheriyan and Sheets, 2018). Thus, there appears regional specific alterations to BLA-mPFC-PAG neuronal networks that must be considered if novel and effective CNS therapeutic strategies are to be realised.

We find that PrL-P neurons alter sensory and affective aspects of neuropathic pain, at least in part, via actions on spinal dorsal horn nociceptive processing. Recently, Huang et al dissected BLA-PrL-PAG circuitry and demonstrated contributions of spinal noradrenergic alpha-2 receptor and serotonergic 5-HT receptor 1/2 signalling to PrL effects on pain-like behaviour in neuropathic rats (Huang *et al.*, 2019). However, expression of these receptors in the spinal ventral horn confounds interpretation of effects on sensory/nociceptive versus motor processing (Shi *et al.*, 1999; Perrier *et al.*, 2013). Here we show that, in neuropathic animals, peripherally evoked spinal dorsal horn wide dynamic range (WDR) neurons are inhibited by PrL-P neuronal activity confirming that the PrL is able to engage descending pain modulatory systems that originate in the PAG. Spinal WDR neurons are a known target of descending modulatory systems and their activity correlates well with both withdrawal reflexes and pain perception (Maixner *et al.*, 1986; You *et al.*, 2003; McMullan and Lumb, 2006a; Drake *et al.*, 2016). It is significant from a therapeutic perspective that the PrL is able to affect nociceptive information early in the ascending pathway, likely prior to extensive integration with other nociceptive / non-nociceptive information which would allow for selective and potent actions on the pain experience and pain state development (Heinricher *et al.*, 2009).

Spinal noradrenergic alpha -2- signalling masks latent mechanical and cold allodynia at early, but not late, time points post tibial nerve injury and shows a remarkably similar chronology to that observed in this study (Hughes *et al.*, 2013). These observations, supported by those of Huang et al, suggests that spinal noradrenaline (NA) release mediates a large part of the PrL analgesic actions in the spinal dorsal horn (Hughes *et al.*, 2013, 2015; Huang *et al.*, 2019). Our findings indicate that the progressive loss of spinal noradrenergic tone in this neuropathic model is due to the loss in top-down executive control from PrL-P neurons but this is yet to be definitively tested. Despite this loss in function, potentiation of spinal NA signalling with reuptake inhibitors can prevent the development of neuropathic pain and reverse neuropathic hypersensitivity in late stage neuropathic animals (Hughes *et al.*, 2015), and NA reuptake inhibitors are currently used to treat neuropathic pain in human patients (Finnerup *et al.*, 2015). Therapeutic strategies aimed at lifting the enhanced feedforward inhibition in the PrL combined with potentiation of spinal NA signalling could provide a novel approach to treat neuropathic pain in humans. Although, targeted approaches are likely necessary as chemo-activation of Locus Coeruleus projections to the spinal dorsal horn and mPFC produce pain relief and conflicting negative affect in neuropathic rats (Hirschberg *et al.*, 2017).

At early post-injury timepoints, chemo-inhibition of PrL-P neurons produced place aversion indicating that loss of cortical control over the PAG and associated DPMS worsens the affective state of injured animals. This change in affective state is likely secondary to effects on spinal nociceptive processing as neuropathic animals show ongoing pain like behaviour and its relief, for instance by stimulating spinal NA receptors, produces place preference in neuropathic rats (King *et al.*, 2009; Hirschberg *et al.*, 2017). However, direct effects of PrL-P neurons on affective processing should not be overlocked given the role of the PAG in fear, anxiety and depression (Tovote, Fadok and Lüthi, 2015; George, Ameli and Koob, 2019). Interestingly, Rozekse et al showed dorsal medial prefrontal cortex projections to the PAG regulate the appropriate expression of aversive memories suggesting that loss of functional communication between the PrL and PAG may lead to generalised aversion and negative affect (Rozeske *et al.*, 2018). The PrL has previously been shown to contribute to pain related anxiety,

deficiencies in reward processing and avoidance behaviour (Lee *et al.*, 2015; Wang *et al.*, 2015; Zhang *et al.*, 2015; Liang *et al.*, 2020). Our findings add to the growing picture of mPFC-PAG communication as a critical regulator in a range of disease relevant features including emotional coping, aversive learning and autonomic control including nociceptive processing and, now, neuropathic pain state development (Franklin *et al.*, 2017; Rozeske *et al.*, 2018; Huang *et al.*, 2019).

In summary, we have identified specific contributions of PrL-P neurons to regulate nociception in healthy animals and charted their dynamic contributions to neuropathic pain state development following injury. Our findings suggest that PrL-P neurons engage descending inhibitory control of the spinal dorsal horn to regulate CNS nociceptive processing and moment to moment noxious threshold to affect behaviour. Following nerve injury, tone in PrL-P neurons initially constrains the spatiotemporal development of neuropathic hypersensitivity but there is a progressive loss in the functional communication between the PrL and PAG as the pain state develops. Our findings aid interpretation of human clinical observations that demonstrate altered functional connectivity between the mPFC and PAG is an important mechanism in the development of chronic pain.

References:

An, X. *et al.* (1998) 'Prefrontal cortical projections to longitudinal columns in the midbrain periaqueductal gray in macaque monkeys.', *The Journal of comparative neurology*, 401(4), pp. 455–79. Available at: http://www.ncbi.nlm.nih.gov/pubmed/9826273.

Apkarian, A. V. *et al.* (2004) 'Chronic back pain is associated with decreased prefrontal and thalamic gray matter density', *Journal of Neuroscience*, 24(46), pp. 10410–10415. doi: 10.1523/JNEUROSCI.2541-04.2004.

Baliki, M. N. *et al.* (2006) 'Chronic pain and the emotional brain: specific brain activity associated with spontaneous fluctuations of intensity of chronic back pain.', *The Journal of neuroscience : the official journal of the Society for Neuroscience*, 26(47), pp. 12165–73. doi: 10.1523/JNEUROSCI.3576-06.2006.

Baliki, M. N. *et al.* (2012) 'Corticostriatal functional connectivity predicts transition to chronic back pain.', *Nature neuroscience*. Nature Publishing Group, 15(8), pp. 1117–9. doi: 10.1038/nn.3153.

Baliki, M. N. and Apkarian, A. V. (2015) 'Nociception, Pain, Negative Moods, and Behavior Selection', *Neuron*. Elsevier Inc., 87(3), pp. 474–491. doi: 10.1016/j.neuron.2015.06.005.

Bannister, K. *et al.* (2015) 'Diffuse noxious inhibitory controls and nerve injury: Restoring an imbalance between descending monoamine inhibitions and facilitations', *Pain*, 156(9), pp. 1803–1811. doi: 10.1097/j.pain.0000000000000240.

Boender, A. J. *et al.* (2014) 'Combined use of the canine adenovirus-2 and DREADD-technology to activate specific neural pathways in vivo.', *PloS one*, 9(4), p. e95392. doi: 10.1371/journal.pone.0095392.

Breivik, H. *et al.* (2006) 'Survey of chronic pain in Europe: prevalence, impact on daily life, and treatment', *Eur J Pain*. 2005/08/13, 10(4), pp. 287–333. doi: S1090-3801(05)00086-8 [pii]10.1016/j.ejpain.2005.06.009.

1 Brooks, J. C. W., Davies, W. E. and Pickering, A. E. (2017) 'Resolving the brainstem contributions to
2 attentional analgesia', *Journal of Neuroscience*, 37(9), pp. 2279–2291. doi:
3 10.1523/JNEUROSCI.2193-16.2016.

4 Chaplan, S. R. *et al.* (1994) 'Quantitative assessment of tactile allodynia in the rat paw', *Journal of*
5 *Neuroscience Methods*, 53(1), pp. 55–63. doi: 10.1016/0165-0270(94)90144-9.

6 Chen, Z. *et al.* (2017) 'Disrupted functional connectivity of periaqueductal gray subregions in episodic
7 migraine', *Journal of Headache and Pain*. The Journal of Headache and Pain, 18(36). doi:
8 10.1186/s10194-017-0747-9.

9 Cheriyan, J. *et al.* (2016) 'Specific targeting of the basolateral amygdala to projectionally defined
10 pyramidal neurons in prelimbic and infralimbic cortex', *eNeuro*, 3(2), pp. 1–13. doi:
11 10.1523/ENEURO.0002-16.2016.

12 Cheriyan, J. and Sheets, P. L. (2018) 'Altered excitability and local connectivity of mPFC-PAG neurons
13 in a mouse model of neuropathic pain Altered excitability and local connectivity of mPFC-PAG
14 neurons in a mouse model of neuropathic pain . Running title : Nerve injury alters mPFC-PAG circui',
15 *J. Neurosci*, 38(20), pp. 4829–4839. doi: 10.1523/JNEUROSCI.2731-17.2018.

16 Cifre, I. *et al.* (2012) 'Disrupted functional connectivity of the pain network in fibromyalgia',
17 *Psychosomatic Medicine*, 74(1), pp. 55–62. doi: 10.1097/PSY.0b013e3182408f04.

18 Denk, F., McMahon, S. B. and Tracey, I. (2014) 'Pain vulnerability: a neurobiological perspective',
19 *Nature Neuroscience*. Nature Publishing Group, 17(2), pp. 192–200. doi: 10.1038/nn.3628.

20 Drake, R. A. R. *et al.* (2016) 'Periaqueductal Grey EP3 Receptors Facilitate Spinal Nociception in
21 Arthritic Secondary Hypersensitivity', *Journal of Neuroscience*, 36(35), pp. 9026–9040. doi:
22 10.1523/JNEUROSCI.4393-15.2016.

23 Drake, R. a R. *et al.* (2014) 'The degree of acute descending control of spinal nociception in an area
24 of primary hyperalgesia is dependent on the peripheral domain of afferent input.', *The Journal of*

physiology, 592(16), pp. 3611–3624. doi: 10.1113/jphysiol.2013.266494.

Edwards, R. R. (2005) 'Individual differences in endogenous pain modulation as a risk factor for chronic pain', *Neurology*, 65(3), pp. 437–443. doi: 10.1212/01.wnl.0000171862.17301.84.

Eippert, F. *et al.* (2009) 'Direct Evidence for Spinal Cord Involvement in Placebo Analgesia', *Science (New York, N.Y.)*, 326, p. 404.

Finnerup, N. B. *et al.* (2015) 'Pharmacotherapy for neuropathic pain in adults: Systematic review, meta-analysis and updated NeuPSig recommendations', *Lancet Neurol*, 14(2), pp. 162–173. doi: 10.1016/S1474-4422(14)70251-0.Pharmacotherapy.

Floyd, N. S. *et al.* (2000) 'Orbitomedial Prefrontal Cortical Projections to Distinct Longitudinal Columns of the Periaqueductal Gray in the Rat', *Journal of Comparative Neurology*, 422, pp. 556–578.

Franklin, T. B. *et al.* (2017) 'Prefrontal cortical control of a brainstem social behavior circuit', *Nat Neurosci*, 20, pp. 260–270. doi: 10.1101/073734.

George, D. T., Ameli, R. and Koob, G. F. (2019) 'Periaqueductal Gray Sheds Light on Dark Areas of Psychopathology', *Trends in Neurosciences*. Elsevier Ltd, 42(5), pp. 349–360. doi: 10.1016/j.tins.2019.03.004.

González-Roldán, A. M. *et al.* (2020) 'Age-Related Changes in Pain Perception Are Associated With Altered Functional Connectivity During Resting State', *Frontiers in Aging Neuroscience*, 12(May), pp. 1–10. doi: 10.3389/fnagi.2020.00116.

Granovsky, Y. (2013) 'Conditioned pain modulation: A predictor for development and treatment of neuropathic pain', *Current Pain and Headache Reports*, 17(9). doi: 10.1007/s11916-013-0361-8.

Hargreaves, K. *et al.* (1988) 'A new and sensitive method for measuring thermal nociception in cutaneous hyperalgesia', *Pain*, 32(1), pp. 77–88. doi: 10.1016/0304-3959(88)90026-7.

Harper, D. E. *et al.* (2018) 'Resting Functional Connectivity of the Periaqueductal Gray is Associated with Normal Inhibition and Pathological Facilitation in Conditioned Pain Modulation', *The Journal of Pain*. Elsevier Inc., 19(6). doi: 10.1016/J.JPAIN.2018.01.001.

Hashmi, J. a. *et al.* (2013) 'Shape shifting pain: chronification of back pain shifts brain representation from nociceptive to emotional circuits', *Brain*, 136(9), pp. 2751–2768. doi: 10.1093/brain/awt211.

Heinricher, M. M. *et al.* (2009) 'Descending control of nociception: Specificity, recruitment and plasticity', *Brain Res Rev*. 2009/01/17, 60(1), pp. 214–225. doi: S0165-0173(08)00147-1 [pii]10.1016/j.brainresrev.2008.12.009.

Hemington, K. S. and Coulombe, M.-A. (2015) 'The periaqueductal gray and descending pain modulation: why should we study them and what role do they play in chronic pain?', *Journal of neurophysiology*, 114(4), pp. 2080–3. doi: 10.1152/jn.00998.2014.

Hirschberg, S. *et al.* (2017) 'Functional dichotomy in spinal-vs prefrontal-projecting locus coeruleus modules splits descending noradrenergic analgesia from ascending aversion and anxiety in rats', *eLife*, 6(Lc), pp. 1–26. doi: 10.7554/eLife.29808.001.

Hnasko, T. S. *et al.* (2006) 'Cre recombinase-mediated restoration of nigrostriatal dopamine in dopamine-deficient mice reverses hypophagia and bradykinesia', *Proceedings of the National Academy of Sciences of the United States of America*, 103(23), pp. 8858–8863. doi: 10.1073/pnas.0603081103.

Huang, J. *et al.* (2019) 'A neuronal circuit for activating descending modulation of neuropathic pain', *Nature Neuroscience*. Springer US, 22(10), pp. 1659–1668. doi: 10.1038/s41593-019-0481-5.

Hughes, S. *et al.* (2015) 'Intrathecal reboxetine suppresses evoked and ongoing neuropathic pain behaviours by restoring spinal noradrenergic inhibitory tone.', *Pain*, 156(2), pp. 328–34. doi: 10.1097/01.j.pain.0000460313.73358.31.

Hughes, S. W. *et al.* (2013) 'Endogenous analgesic action of the pontospinal noradrenergic system

spatially restricts and temporally delays the progression of neuropathic pain following tibial nerve injury.', *Pain*. International Association for the Study of Pain, 154(9), pp. 1680–90. doi: 10.1016/j.pain.2013.05.010.

Jensen, K. B. *et al.* (2012) 'Patients with fibromyalgia display less functional connectivity in the brain's pain inhibitory network', *Molecular Pain*, 8(1), p. 32. doi: 10.1186/1744-8069-8-32.

Keay, K. A. and Bandler, R. (2001) 'Parallel circuits mediating distinct emotional coping reactions to different types of stress', *Neurosci Biobehav Rev*. 2002/01/22, 25(7–8), pp. 669–678. doi: S0149763401000495 [pii].

King, T. *et al.* (2009) 'Unmasking the tonic-aversive state in neuropathic pain.', *Nature neuroscience*, 12(11), pp. 1364–6. doi: 10.1038/nn.2407.

Kiritoshi, T., Ji, G. and Neugebauer, V. (2016) 'Rescue of Impaired mGluR5-Driven Endocannabinoid Signaling Restores Prefrontal Cortical Output to Inhibit Pain in Arthritic Rats', *Journal of Neuroscience*, 36(3), pp. 837–850. doi: 10.1523/JNEUROSCI.4047-15.2016.

Lee, M. *et al.* (2015) 'Activation of Corticostriatal Circuitry Relieves Chronic Neuropathic Pain', *Journal of Neuroscience*, 35(13), pp. 5247–5259. doi: 10.1523/JNEUROSCI.3494-14.2015.

Legrain, V. *et al.* (2011) 'The pain matrix reloaded: a salience detection system for the body.', *Progress in neurobiology*, 93(1), pp. 111–24. doi: 10.1016/j.pneurobio.2010.10.005.

Leith, J. L. *et al.* (2014) 'Periaqueductal grey cyclooxygenase-dependent facilitation of C-nociceptive drive and encoding in dorsal horn neurons in the rat.', *J Physiol*, 592(22), pp. 5093–5107.

Liang, H. Y. *et al.* (2020) 'nNOS-expressing neurons in the vmPFC transform pPVT-derived chronic pain signals into anxiety behaviors', *Nature Communications*. Springer US, 11(1), pp. 1–18. doi: 10.1038/s41467-020-16198-5.

Lorenz, J. *et al.* (2002) 'A unique representation of heat allodynia in the human brain.', *Neuron*,

35(2), pp. 383–93. Available at: http://www.ncbi.nlm.nih.gov/pubmed/12160755.

Maixner, W. *et al.* (1986) 'Wide-dynamic-range dorsal horn neurons participate in the encoding process by which monkeys perceive the intensity of noxious heat stimuli', *Brain Research*, 374(2), pp. 385–388. doi: 10.1016/0006-8993(86)90435-X.

Mantyh, P. W. (1983) 'Connections of midbrain periaqueductal gray in the monkey. II. Descending efferent projections.', *Journal of neurophysiology*, 49(3), pp. 582–94. Available at: http://www.ncbi.nlm.nih.gov/pubmed/6300351.

McMullan, S. and Lumb, B. M. (2006a) 'Midbrain control of spinal nociception discriminates between responses evoked by myelinated and unmyelinated heat nociceptors in the rat', *Pain*. 2006/05/03, 124(1–2), pp. 59–68. doi: S0304-3959(06)00181-3 [pii]10.1016/j.pain.2006.03.015.

McMullan, S. and Lumb, B. M. (2006b) 'Spinal dorsal horn neuronal responses to myelinated versus unmyelinated heat nociceptors and their modulation by activation of the periaqueductal grey in the rat', *J Physiol*. 2006/08/19, 576(Pt 2), pp. 547–556. doi: jphysiol.2006.117754 [pii]10.1113/jphysiol.2006.117754.

Meda, K. S. *et al.* (2019) 'Microcircuit Mechanisms through which Mediodorsal Thalamic Input to Anterior Cingulate Cortex Exacerbates Pain-Related Aversion', *Neuron*. Elsevier Inc., 102(5), pp. 944-959.e3. doi: 10.1016/j.neuron.2019.03.042.

Millan, M. J. (2002) 'Descending control of pain', *Prog Neurobiol*. 2002/05/30, 66(6), pp. 355–474. doi: S0301008202000096 [pii].

Mills, E. P. *et al.* (2018) 'Brainstem pain-control circuitry connectivity in chronic neuropathic pain', *Journal of Neuroscience*, 38(2), pp. 465–473. doi: 10.1523/JNEUROSCI.1647-17.2017.

Mitrić, M. *et al.* (2019) 'Layer- and subregion-specific electrophysiological and morphological changes of the medial prefrontal cortex in a mouse model of neuropathic pain', *Scientific Reports*, 9(1), pp. 1–13. doi: 10.1038/s41598-019-45677-z.

Oliva, V. *et al.* (2020) 'Parallel cortical-brainstem pathways to attentional analgesia'. Elsevier Inc., 226(June 2020). doi: 10.1101/2020.02.20.955161.

Ossipov, M. H., Dussor, G. O. and Porreca, F. (2010) 'Central modulation of pain', *The Journal of Clinical Investigation*, 120(11), pp. 3779–3787. doi: 10.1172/JCI43766.reduced.

Perrier, J.-F. *et al.* (2013) 'Modulation of the Intrinsic Properties of Motoneurons by Serotonin', *Current Pharmaceutical Design*, 19(24), pp. 4371–4384. doi: 10.2174/13816128113199990341.

Richardson, D. *et al.* (2015) 'Tibial Nerve Transection (TNT) Model of Neuropathic Pain in the Rat', *Figshare*. doi: 10.6084/M9.FIGSHARE.1373622.V1.

Rozeske, R. R. *et al.* (2018) 'Prefrontal-Periaqueductal Gray-Projecting Neurons Mediate Context Fear Discrimination', *Neuron*, 97(4), pp. 898-910.e6. doi: 10.1016/j.neuron.2017.12.044.

Segerdahl, A. R. *et al.* (2018) 'A brain-based pain facilitation mechanism contributes to painful diabetic polyneuropathy', *Brain*, 141(2), pp. 357–364. doi: 10.1093/brain/awx337.

Shi, T. J. *et al.* (1999) 'Distribution of alpha2-adrenoceptor mRNAs in the rat lumbar spinal cord in normal and axotomized rats.', *Neuroreport*, 10(13), pp. 2835–9. Available at: http://www.ncbi.nlm.nih.gov/pubmed/10511449.

Staud, R. (2013) 'Abnormal endogenous pain modulation is a shared characteristic of many chronic pain conditions', *Expert Rev Neurother*, 12(5), pp. 577–585. doi: 10.1586/ern.12.41.Abnormal.

Sternson, S. M. and Roth, B. L. (2014) 'Chemogenetic Tools to Interrogate Brain Functions.', *Annual review of neuroscience*, 37, pp. 387–407. doi: 10.1146/annurev-neuro-071013-014048.

Tovote, P. *et al.* (2016) 'Midbrain circuits for defensive behaviour', *Nature*. Nature Publishing Group, 534(7606), pp. 206–212. doi: 10.1038/nature17996.

Tovote, P., Fadok, J. P. and Lüthi, A. (2015) 'Neuronal circuits for fear and anxiety', *Nature Reviews Neuroscience*. Nature Publishing Group, 16(6), pp. 317–331. doi: 10.1038/nrn3945.

Tracey, I. and Mantyh, P. W. (2007) 'The cerebral signature for pain perception and its modulation', *Neuron*. 2007/08/07, 55(3), pp. 377–391. doi: S0896-6273(07)00533-8 [pii]10.1016/j.neuron.2007.07.012.

Vanegas, H. and Schaible, H. G. (2004) 'Descending control of persistent pain: inhibitory or facilitatory?', *Brain Res Brain Res Rev*. 2004/12/02, 46(3), pp. 295–309. doi: S0165-0173(04)00102-X [pii]10.1016/j.brainresrev.2004.07.004.

Wager, T. D. *et al.* (2004) 'Placebo-Induced Changes in fMRI in the Anticipation and Experience of Pain', *Science*, 303(5661), pp. 1162–1167. doi: 10.1126/science.1093065.

Wang, G.-Q. *et al.* (2015) 'Deactivation of excitatory neurons in the prelimbic cortex via Cdk5 promotes pain sensation and anxiety', *Nature Communications*, 6(May), p. 7660. doi: 10.1038/ncomms8660.

Wanigasekera, V. *et al.* (2018) 'Disambiguating pharmacological mechanisms from placebo in neuropathic pain using functional neuroimaging', *British Journal of Anaesthesia*. Elsevier Ltd, 120(2), pp. 299–307. doi: 10.1016/j.bja.2017.11.064.

Waters, A. J. and Lumb, B. M. (2008) 'Descending control of spinal nociception from the periaqueductal grey distinguishes between neurons with and without C-fibre inputs', *Pain*. 2007/05/01, 134(1–2), pp. 32–40. doi: S0304-3959(07)00139-X [pii]10.1016/j.pain.2007.03.025.

Wiech, K. *et al.* (2014) 'Dissociable Neural Mechanisms Underlying the Modulation of Pain and Anxiety? An fMRI Pilot Study.', *PloS one*, 9(12), p. e110654. doi: 10.1371/journal.pone.0110654.

Wiech, K. and Tracey, I. (2009) 'The influence of negative emotions on pain: behavioral effects and neural mechanisms.', *NeuroImage*. Elsevier Inc., 47(3), pp. 987–94. doi: 10.1016/j.neuroimage.2009.05.059.

Yarnitsky, D. (2010) 'Conditioned pain modulation (the diffuse noxious inhibitory control-like effect): Its relevance for acute and chronic pain states', *Current Opinion in Anaesthesiology*, 23(5), pp. 611–

615. doi: 10.1097/ACO.0b013e32833c348b.

You, H.-J. *et al.* (2003) 'Simultaneous recordings of wind-up of paired spinal dorsal horn nociceptive neuron and nociceptive flexion reflex in rats.', *Brain research*, 960(1–2), pp. 235–45. Available at: http://www.ncbi.nlm.nih.gov/pubmed/12505677.

Yu, R. *et al.* (2014) 'Disrupted functional connectivity of the periaqueductal gray in chronic low back pain.', *NeuroImage. Clinical*. Elsevier B.V., 6, pp. 100–8. doi: 10.1016/j.nicl.2014.08.019.

Zhang, F. *et al.* (2010) 'Optogenetic interrogation of neural circuits: technology for probing mammalian brain structures.', *Nature protocols*, 5(3), pp. 439–56. doi: 10.1038/nprot.2009.226.

Zhang, Z. *et al.* (2015) 'Role of Prelimbic GABAergic Circuits in Sensory and Emotional Aspects of Neuropathic Pain.', *Cell reports*. The Authors, pp. 1–8. doi: 10.1016/j.celrep.2015.07.001.

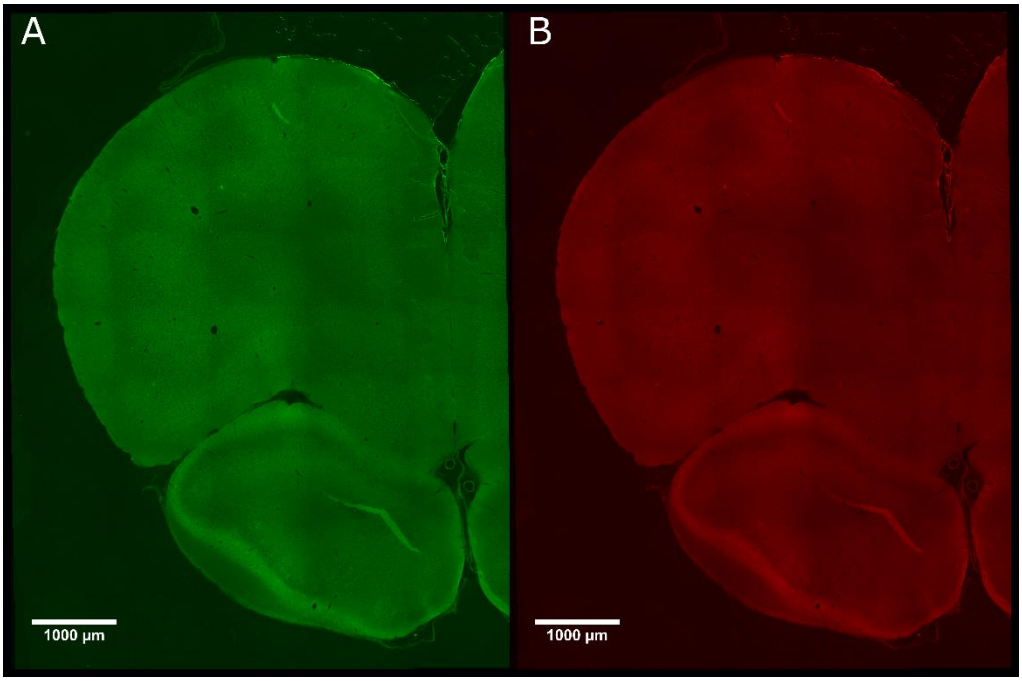

Supplementary Figure 1. There was negligible expression of ChR2-EYP and hM4Di-mCherry in control animals that did not receive CAV-CMV-CRE into the periaqueductal grey. Photomicrograph of mPFC from showing negligible expression of ChR2-EYFP (**A**) or hM4Di-mCherry (**B**) in PrL.Control rats.

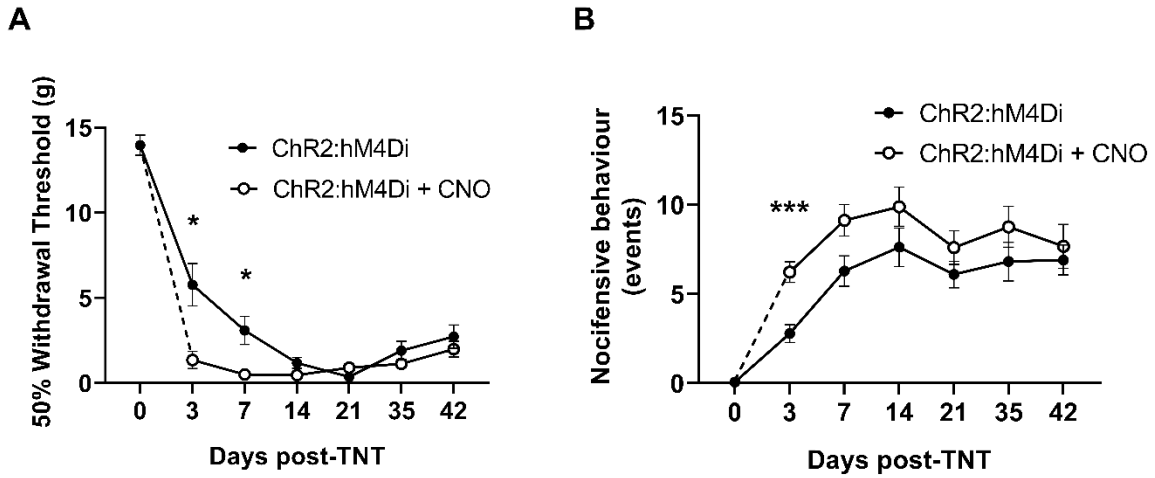

Supplementary Figure 2. Chemo-inhibition of PrL-P neurons affects nocicfensive behaviour in early but not late timepoints post injury in neuropathic animals. A – In $TNT^{PrL.ChR2:hM4Di}$ rats systemic delivery of CNO (2.5mg.kg^{-1} i.p.) significantly reduces mechanical withdrawal threshold at 3 and 7 days post injury on the ipsilateral (injured) hind-paw (Mixed Model (REML), Fixed effects CNO $F(1,28) = 7.26$ $p=0.002$, Time x CNO $F(5,95) =4.92$ $p=0.0005$, Sidaks post-test *$p<0.05$, n= 16). **B** – In $TNT^{PrL.ChR2:hM4Di}$ rats ,systemic delivery of CNO (2.5mg.kg^{-1} i.p.) significantly increases the cold (acetone) evoked nocicfensive events at 3 days post injury on the ipsilateral (injured) hind-paw (Mixed Model (REML), Fixed effects CNO $F(1,30)=6.3$ $p=0.02$, Time x CNO $F(5,98)=0.6$ $p=0.70$, Sidak's post-test ***$p=0.0006$, n= 16).

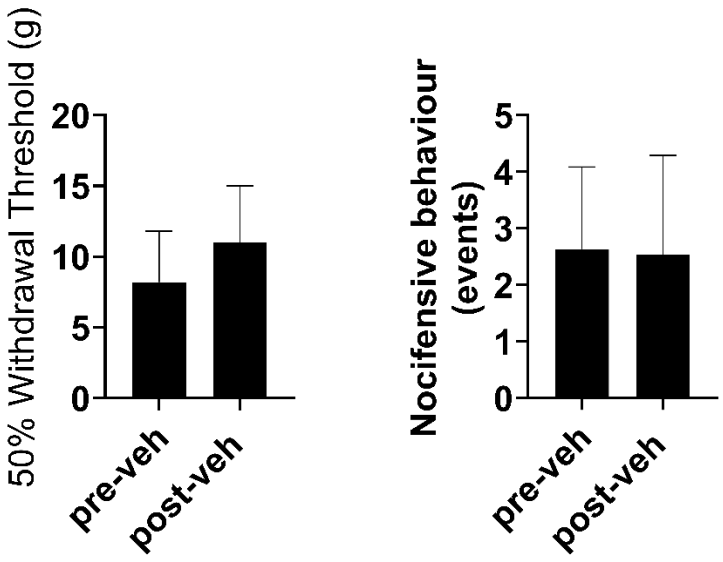

Supplementary Figure 3. Delivery of vehicle does not affect sensitisation in TNT$^{PrL.ChR2:hM4Di}$ rats at 7 days post-TNT. Delivery of Vehicle (sterile saline with 5% DMSO, i.p.) does not alter mechanical withdrawal thresholds (Paired t-test 0.4, n=3) (**A**) or cold evoked nocicfensive behaviour (Paired t-test 0.86 (**B**) in TNT$^{PrL.ChR2:hM4Di}$ rats (n=3).